Formulation, Optimization, in Vitro and in Vivo Investigation of Ketoprofen - Fumaric Acid Co-crystal for the Solubility Enhancement of Ketoprofen

Meenakshi Bhatia
Guru Jambheshwar University of Science & Technology
Ashwani Kumar
Guru Jambheshwar University of Science & Technology
Vikas Verma
Guru Jambheshwar University of Science & Technology
Snehlata Yadav
Indira Gandhi University Meerpur
SUNITA DEVI (sunitamechu1504@gmail.com)
Guru Jambheshwar University of Science & Technology

Research Article

Keywords: ketoprofen, fumaric acid, Co-crystal, non-covalent interactions, solubility

Posted Date: October 12th, 2021

DOI: https://doi.org/10.21203/rs.3.rs-905168/v1

Abstract

The present piece of research work is framed as improving the solubility of ketoprofen by forming co-crystal using fumaric acid as a coformer. Co-crystal of ketoprofen and fumaric acid were prepared by simple solvent assisted grinding. The independent variables i.e. drug and coformer were mixed in 1:1 molar ratio and dependent variables were assumed to be solubility and % drug release. Differential scanning calorimetry, fourier transform infrared spectroscopy, X-ray diffraction, nuclear magnetic resonance and scanning electron microscopy techniques were used to characterize the preparation of optimized batch of co-crystal and further, evaluated for *in-vitro* and *in-vivo* anti-inflammatory and analgesic activities. Based on results of solubility and dissolution rate studies the drug showed 4-5 fold improvement in both the properties on co-crystallisation. The values of Gibbs free energy are negative at all levels of carrier demonstrating spontaneity of drug solubilization process. The IC_{50} value of optimized batch of co-crystal formulation and pure drug was observed as 327.33 µg/ml and 556.11 µg/ml, respectively, demonstrating that co-crystal formulation possesses more percentage protection against protein denaturation than the drug ketoprofen. *In-vivo* (anti-inflammatory and analgesic) activities revealed that optimized batch of co-crystal formulation delivered a rapid pharmacological response in wistar rats and albino mice when compared with standard drug.

Introduction

Numerous strategies to improve bioavailability of drugs with poor/low solubility include drug micronization in to amorphous form [1], complexation with hydrophilic carrier [2–4], solid dispersion [5, 6], micellar solubilization [7], nanoparticle technology [8–11], self-emulsifying drug delivery systems [12–14], salt formation [15], liposomes [16], nanostructured lipid carriers (NLC) [17, 18], prodrug [19] and formation of co-crystal [20–25] etc. However, there are disadvantages associated with these techniques like agglomeration, instability during storage, requirement of advanced/or sophisticated instruments, tacky product etc. Therefore, co-crystallization appears to be a potential method for improving the solubility, dissolution and thus bioavailability of crystalline materials being a direct, viable, economical and green method. Co-crystal is defined as a multicomponent crystalline material possessing two or more molecules (i.e. drug and coformers) that are held together by noncovalent interactions in the same crystal lattice [26]. Co-crystallization can appreciably reorganize the physiochemical properties of active pharmaceutical ingredient (API) by introducing a coformer that interconnected with the target API in a defined stoichiometric ratio through intermolecular interactions [27]. The enhancement in solubility is explained by the two step mechanism as first the solute molecules are released from the crystal lattice followed by the solvation of released molecules. Also the Gibbs free energy (ΔG) associated with this system ($\Delta G_{solution}$) involves free energy allied with release of solute molecules from the lattice i.e. ΔG_{lat} and solvation barrier (ΔG_{solv}) that may be attributed as:

$$\Delta G_{solution}=\Delta G_{lat}+\Delta G_{solv} \quad (1)$$

At the moment, the free energy equated with lattice interaction and solvation barrier because trivial, the dissolution of co-crystal is improved due to drop free energy change for solubilization [28, 29].

Here, in this study ketoprofen, a nonsteroidal anti-inflammatory drug, belonging to the BCS class II was selected as a model drug that pertain low solubility and high permeability. Ketoprofen works by inhibiting the enzyme cyclooxygenase-I and II, resulting in decreased production of precursors of prostaglandins and thromboxanes,

thereby, displaying antipyretic, anti-inflammatory and analgesic activities. Nanosuspensions with Phosphol-ipon 80 [30], soild dispersion [31], microemulsion-based gel [32], emulgels [33], nanoparticles [34–36], solid lipid nanoparticles [37], nanostructured lipid carriers [38], prodrugs [39], micro and nanocomposites with PLGA [40] and liquisolid [41] etc. have already been used to increase the solubility of ketoprofen. However, co-crystal of ketoprofen with nicotinamide by grinding method are reported in literature that depicted higher anti-inflammatory activity [42].

The dicarboxylic acid *viz.* fumaric acid was selected as co-crystal coformer in the present study. Fumaric acid is a popular coformer that has been widely explored for the production of co-crystal of different active pharmaceutical ingredients like glycine [43], meloxicam [44], (DL)-phenylalanine [45], adenine [46], 5-Fluorocytosine [47], arginine [48] berberine chloride [49], Ketoconazole [50] etc. The ketoprofen and fumaric acid were selected on the basis of the pK_a rule. Fumaric acid exhibits an aqueous solubility of ~0.6 g/l at 24°C and has pK_a value of 3.03 whereas pK_a value for ketoprofen is 3.88 and the value of ΔpK_a ($pK_{aacid} - pK_{abase}$) is − 0.85. According to Bhogala et al., at negative values of ΔpK_a co-crystal formation is expected [51].

There is no study reported on co-crystal formation of ketoprofen with fumaric acid. In the present piece of research-work formation of ketoprofen co-crystal with fumaric acid is described with the objective to enhance aqueous solubility of drug utilizing simple and reproducible technique of solvent-assisted grinding. The preparation of co-crystal was achieved as per experimental design protocol as recommended by the 2-factor, 3 level CCD (central composite experimental design, Design Expert software version 11.0). The solubility, Gibbs free energy, entrapment efficiency and *in-vitro* drug release for each batch was determined and numerically optimized. The optimized batch as suggested by design expert was characterized by FT-IR, DSC, XRD, SEM and NMR studies. The evaluation of optimized batch was carried out by *in-vitro*/ *in-vivo* anti-inflammatory and analgesic activity employing suitable animal models like rat paw edema and tail flick methods. Further, the mechanism of drug release was determined by fitting the release data in various release kinetics models.

Experimental

Materials

Ketoprofen (ket) was received as a gift sample from Infinity Laboratories Pvt. Ltd (Behra, India). Fumaric acid (FA) was supplied by Central Drug House (P) Ltd., New Delhi. Ethanol, potassium chloride, di-sodium hydrogen orthophosphate, potassium di-hydrogen orthophosphate, sodium chloride and carrageenan were obtained from Hi-Media lab. Pvt. Ltd. All other chemicals & reagents were of analytical grade and used as received. The chemical structures of ketoprofen and fumaric acid were obtained from pubchem database [https://pubchem.ncbi.nlm.nih.gov].

Method

Preparation of ketoprofen-fumaric acid co-crystal

Ketoprofen-fumaric acid co-crystal (Ket-FACo) were prepared by the simple solvent-assisted grinding technique as reported earlier [52, 53]. Ketoprofen and fumaric acid were used in stoichiometrically equal ratio and after carefully weighing were ground using a mortar and pestle for 30 minutes with the dropwise addition of ethanol. The powder was dried, preserved in airtight vials and stored in a desiccator till further use.

Experimental Design

The preparation of co-crystals using ketoprofen and fumaric acid was optimized using 2-factor, 3 level central composite experimental design. The concentration of ketoprofen (254.29-508.58 mg) (X_1) and concentration of FA (116.07-232.14 mg) (X_2) were designated as formulation variables whereas the % drug release and solubility (µg/ml) were selected as response variables (Table I) and each of the independent variable was considered at 3 levels (-1, 0, and 1). Experimental design and statistical analysis of the data was realized by Design Expert software (version 11.0).

Solubility studies

To determine the solubility of ketoprofen and each batch of Ket-FACo formulations carrying drug equivalent to 5 mg and pure drug (5 mg) was dispersed in 20 ml of distilled water and phosphate buffer solution pH-7.4, separately and were kept on continuous shaking at room temperature for 48 h. The obtained solution was then filtered by 0.45µm millipore filter paper and the drug content was measured by taking absorbance at 260 nm using *uv-vis* spectrophotometer. The amount of drug was measured using the calibration curve in water [5].

The Gibbs free energy of transfer (ΔG) of ketoprofen present in different batches of co-crystal is determined using equation 2.

$$\Delta G = -2.303RT \log S_o/S_s \qquad (2)$$

S_o is the solubility of the co-crystal in water and Ss is the solubility of pure drug in water,

R = 8.31 J $k^{-1}mol^{-1}$ and T = 298.15°C.

Percentage Drug content

To ascertain the drug content of every batch of Ket-FACo formulation, co-crystal equivalent to 5 mg were weighed and dissolved separately in 25 ml of phosphate buffer (pH 7.4) in volumetric flask with continuous stirring for 24 h on a magnetic stirrer [54], after proper dilutions, drug content was determined using *uv-vis* spectrophotometrically at 260 nm.

The following equation was used to calculated Total Drug Content (TDC)

$$\mathrm{Totaldrugcontent}\,(\backslash\%) = \frac{\mathrm{Weightofdruginco-crystal}}{\mathrm{Weightofco-crystal}} \times 100 \quad (3)$$

In vitro drug release profile

In vitro dissolution studies of pure drug (Ketoprofen) and each batch of Ket-FACo formulation containing Ketoprofen equal to 20mg were conducted in 900ml PBS (phosphate buffer solution, pH-7.4) at 37 ± 0.5°C with constant stirring speed of 50 rpm. The powder was dispersed over the dissolution medium. Aliquots of sample (5ml) were withdrawn at different time intervals for 1 h and restored with an equal volume of the dissolution medium to keep sink conditions in the course of the experiment. The 0.45µm milipore filters was used for the sample filtration and the drug concentration in the samples was determined by measuring the absorbance of the samples at a wavelength of 260 nm using the *uv–vis* spectrophotometer followed by determination of mechanism of release by fitting the release rate data in various release kinetic models [6].

In vitro drug release profile

In vitro dissolution studies of pure drug (Ketoprofen) and each batch of Ket-FACo formulation containing Ketoprofen equal to 20mg were conducted in 900ml PBS (phosphate buffer solution, pH-7.4) at 37±0.5^{o}C with constant stirring speed of 50 rpm. The powder was dispersed over the dissolution medium. Aliquots of sample (5ml) were withdrawn at different time intervals for 1 h and restored with an equal volume of the dissolution medium to keep sink conditions in the course of the experiment. The 0.45µm milipore filters was used for the sample filtration and the drug concentration in the samples was determined by measuring the absorbance of the samples at a wavelength of 260 nm using the *uv–vis* spectrophotometer followed by determination of mechanism of release by fitting the release rate data in various release kinetic models [6].

Characterization

Fourier Transform Infrared Spectroscopy (FT-IR) analysis

FT-IR analysis was used for the interaction between drug and carrier. FTIR spectral analysis of ketoprofen, fumaric acid and optimized batch of Ket-FACo formulation was done by FT-IR Perkin-Elmer, Spectrum, US spectrophotometer and the spectrum was documented in the wavelength region of 4000cm^{-1} to 400 cm^{-1} using KBr pellet method.

X-ray diffraction analysis (XRD) analysis

The XRD spectra of ketoprofen, fumaric acid and optimized batch of Ket-FACo formulation were obtained using an X-ray diffractometer (Miniflex 2, Rigaku, Japan) at room temperature and at 30kV. The scanning diffraction angle (2θ) ranging from 0^{o} to 80^{o}. The Miller index (d_{hkl}) is used to establish direction and plane in the crystal and is determined using Bragg's equation (Eq. 4).

$$\mathrm{n}\lambda = 2\mathrm{dhkl}Sin\theta$$

4

Here λ and n denote the wavelength (1.5418Å) and order (n = 1, first order), respectively; θ is the Bragg's angle.

Differential scanning calorimetry (DSC)

DSC thermograms of ketoprofen, Fumaric acid and optimized batch of Ket-FACo formulation were recorded using DSC (Mettler Toledo, Switzerland), the samples were heated within the temperatures range of 20-400°C with a scanning rate of 10°C/min in aluminum pans under nitrogen flow at a rate of 50 ml/min.

Scanning electron microscopy (SEM)

The surface morphology and shape of optimized batch of Ket-FACo formulation was observed using scanning electron microscope (JSM-6100 scanning microscopy, Japan).

Nuclear Magnetic Resonance (NMR) Spectroscopy

The NMR spectra of ketoprofen, fumaric acid and optimized batch of Ket-FACo formulation after dissolving in DMSO-d_6 were examined using Bruker Avance AV 400 NMR spectrometer (Bruker, Karlsruhe, Germany) to get

solution ^{13}C NMR data at a temperature of 293 K using Tetramethylsilane (TMS) as an internal standard [55]. Data was interpreted using Mnova program (Mestrelab Research, Santiago de Compostela, Spain).

Stability studies

The optimized batch of co-crystal was kept for the accelerated stability studies according to ICH guidelines (40 ± 2 ^{o}C and 75 ± 5% RH) for a period of 6 months in a stability chamber. The samples were placed in hermetically sealed vials containing rubber plugs and aluminum bung. The stored co-crystal were taken out after 6 months and evaluated for the drug content (according to the method described in earlier section of drug content, *n=3*) and for any physical changes [47].

Biological Evaluation of Ket-FACo

In-vitro anti-inflammatory activity

Egg albumin denaturation method was used to determine *in-vitro* anti-inflammatory activity of drug ketoprofen and optimized batch of Ket-FACo [56–58]. The mixtures containing of fresh hen's egg albumin (0.2ml), Phosphate buffered saline 7.4 (2.8ml) and different concentrations of Ket-FACo formulation (2 ml, containing ketoprofen equivalent to 10 mg) (125, 250, 500, 750 & 1000 µg/ml in Dimethyl sulfoxide as solvent). The mixture was placed in an incubator at a temperature of 37 ± 2 ^{o}C for 20 min incubation followed by heating at 70^{o}C. After cooling at room temperature, the absorbance measured at λ_{max} of 660nm to determine % inhibition. Similar procedure was done for the drug (ketoprofen) with the similiar concentrations as engaged for the formulation as a reference or control. The percentage protection from protein denaturation was calculated as per Eq. 5

% protection from denaturation= $\frac{Abs.of control - Abs.of sample}{Abs.of control}$ X 100 (5)

The half maximal inhibitory concentration (IC_{50}) values of ketoprofen and optimized formulation was calculated by nonlinear regression analysis.

In-vivo carrageenan-induced anti-inflammatory activity

The protocol with registration no. CPCSEA Reg. no-IAEC/2021/10–19 was approved for animal study by the Animal Ethical Committee, Guru Jambheshwar University of Science and Technology, Hisar, India. Wistar rats (150–180 g) were distributed into three groups comprising of six animals each. Group I (control treated) with carrageenan was kept as control, Group II (standard drug) was treated with drug-ketoprofen (10 mg/kg) and Group III (test compound) was treated with Ket-FACo (equivalent to ketoprofen 10 mg/kg body weight) that is administrated orally. 1% suspension of carrageenan (0.1 ml) in normal saline, was administered as subplantar injection in the left hind paw of albino wistar rats, after 1 h of oral administration of the test materials. The paw volume was measured using vernier caliper at 1, 2, 3, 4 and 5 h after the carrageenan injection. The % inhibition in paw volume was calculated using Eq. 6,

$$\%inibition = \frac{Vc - Vt}{Vc} \times 100$$

6

Where V_c and V_t is the inflammatory increase in paw volume control group and test group respectively [59].

Analgesic activity (Tail Flick Method)

Tail flick method was used to measure analgesic activity using a radiant type analgesiometer. Three different groups (control, test and standard) of Swiss albino mice (25-30g) containing six mice each group were taken for study. The tail flick reaction time for each animal was recorded six times before administering the drug and the mean was used as predrug reaction time. A dose of the standard drug (Ketoprofen) and test compound (optimized batch of Ket-FACo) containing ketoprofen equivalent to 5 mg/kg of body weight in 0.9% w/v sterile saline was orally administered to mice. After administration of the drug, the tail flick reaction time was measured at 0, 1, 2, 3, 4 and 5 hrs.

% Analgesic activity (PAA) was calculated as per Eq. 7.

$PAA= (T_2-T_1)/T_1 \times 100$ (7)

Where T_1 are reaction time in second before treatment of drug(s) and T_2 are reaction time in second after treatment of drug(s) [60, 61]. Data was analyzed by one-way ANOVA followed by Tukey's post-hoc test and statistically was denoted as P value.

Results And Discussion

The preparation of co-crystal using ketoprofen and fumaric acid was optimized using 2-factor, 3 level CCD. The concentration of ketoprofen (X_1) and concentration of fumaric acid (X_2) were designated as formulation variables whereas the % drug release and solubility (µg/ml) were picked as response variables. The TDC of different batches of ket-FACo was found to be between 94.48 to 97.81 %, thus depicting that handsome amount of drug has been loaded and also no physical changes were observed during stability studies and even after six months. In different batches of ket-FACo solubility in phosphate buffer (PBS pH-7.4) values range from 29.08 to 10.63 µg/ml whereas ketoprofen solubility was found to be 3.64 µg/ml.

As presented in Table 1, solubility of ket-FACo varied in the range of 30.68-57.44µg/ml. The pure ketoprofen dispensed a solubility of 11.24 µg/ml in water at room temperature.

Table 1. Formulation parameters and responses for central composite experimental design.

Batch	Conc. Of Ketoprofen (mg)	Conc. Of Fumaric acid (mg)	Solubility (µg/ml)	Solubility in PBS pH-7.4 (µg/ml)	ΔG (KJ/MOL)	% Drug release in 60 min.	Drug content (%)
F1	254.29	116.07	30.68±0.01	10.63±0.32	-3.49	62.21±0.03	95.89±0.06
F2	508.58	116.07	42.04±0.03	18.36±0.12	-1.92	70.01±0.05	95.66±0.01
F3	254.29	232.14	48.3±0.01	23.39±0.02	-3.04	71.94±0.02	95.33±0.04
F4	508.58	232.14	57.44±0.05	29.08±08	-2.68	83.68±0.01	97.81±0.01
F5	254.29	174.10	45.97±0.2	21.59±0.22	-2.54	70.52±0.06	96.39±0.06
F6	508.58	174.10	51.08±0.3	28.46±0.13	-3.19	80.59±0.07	95.60±001
F7	381.43	116.07	36.47±0.1	15.16±0.41	-3.32	66.52±0.02	95.04±0.02
F8	381.43	232.14	53.66±0.09	28.52±0.17	-2.93	79.71±0.04	97.47±0.07
F9	381.43	174.10	49.08±0.08	27.46±0.27	-3.36	75.54±0.05	97.25±0.03
F10	381.43	174.10	48.14±0.4	26.94±0.31	-3.08	75.04±0.2	95.53±0.05
F11	381.43	174.10	49.51±0.04	27.67±0.29	-3.04	75.59±0.3	94.88±0.01
F12	381.43	174.10	50.23±0.06	26.54±1.1	-3.15	73.52±0.1	94.48±0.06
F13	381.43	174.10	50.16±0.03	26.83±0.11	-3.12	73.02±0.03	96.35±0.08
Ketoprofen			11.24±0.03	3.64±0.14		23.05±0.01	

All values are expressed as mean ± S.D., n=3.

Table 1 shows the results of solubility of different batches of Ket-FACo organized according to design protocol. The responses produced were fitted into several polynomial models using CCD. The response solubility was fitted greatest into quadratic model with none transformation of the data. The polynomial models for the responses solubility (Y_1) can also be expressed by the equation (8) with determination correlation (R^2) of 0.9659.

$$Y_1 = 49.36+4.27X_1+8.37X_2-0.5550X_1X_2-0.6822X_1^2-4.14X_2^2 \quad (8)$$

Table 2 summarizes the results of ANOVA on the solubility and % drug release response surface model, demonstrated that model was found significant with lack of fit as non-significant. Adequate precision of solubility is found to be 28.33 indicates an adequate signal. The adequate precision measuring signal to noise ratio (greater than 4) is desirable. Fig. 1 (a) show the collective effect of concentration of ketoprofen and fumaric acid on solubility. It may be reckoned from the plots that a curvilinear relationship exists between independent and dependent variables. It is also inferred from the plot that higher level of ketoprofen and fumaric acid results in increase in solubility. However, the effect of the concentration of fumaric acid (X_2) seems to be more pronounced as compared to the concentration of ketoprofen (X_1). This increase in solubility may be due to formation of soluble complex between ketoprofen and fumaric acid. Fumaric acid presents higher solubility than the drug that comes out of the crystal lattice. The drug in co-crystal get supersaturated in aqueous medium and possesses more energy as compared to crystalline phase, thereby, exhibit marked increase in solubility than the pure drug.

In vitro drug release

Results of *in-vitro* drug release (Table 1) revealed that 62.21 to 83.68% and 23.50% of ketoprofen got released from different batches of Ket-FACo and pure drug solution respectively, in 1 h study. This rise in percentage drug release from Ket-FACo as compared to pure drug may be associated to the solubility data. As previously mentioned that the fumaric acid form the soluble complex with the drug and thereby increase the drug wettability that leads to a better solubility and further heads towards better rate of drug release. The adjusted polynomial equation obtained for the *in-vitro* drug release (Y_2) is shown in equation 9 with determination correlation of adjusted R^2 of 0.958 and predicted R^2 of 0.905. The predicted is in reasonable agreement with the adjusted R^2 with a difference less than 0.2.

$$Y_2=74.84+4.93X_1+6.10X_2+0.985X_1X_2-0.0336X_1^2-2.47X_2^2 \quad (9)$$

Table 2 recapitulating the results of ANOVA of *in-vitro* release data on response surface model fitted best in quadratic model (after none transformation of the data). The responses observed were fitted into different polynomials models using the experimental design. Adequate precision of *in-vitro* drug release is found to be 25.57 indicates an adequate signal.

Table 2. Model summary statistics.

	Model					Lack of Fit	
Response factor(Y)	**F-value**	**Prob.>F**	**R^2**	**Adeq.Prec.**	**C.V (%)**	**F-value**	**Prob.>F**
Y_1	69.00	<0.0001	0.9659	28.33	2.79	4.09	0.1035
Y_2	56.65	<0.0001	0.975	25.57	1.60	0.937	0.501

To attain stability a natural tendency to acquire minimum Gibbs energy is always there. All the values of ΔG are negative (Table 1) at all levels of carrier demonstrating spontaneity of drug solubilization process.

Optimization

The optimization equations 8 and 9, involving the response and independent factors were assembled based on a quadratic model. To the responses *i.e.* solubility and *in-vitro* drug release the desirability function was applied with constraints to obtain the higher level of both, the batch F4 comes out to be optimized batch. In this fashion, the formulation containing fumaric acid (228.82mg) as coformer and drug content (508.58 mg) with addition of ethanol, established the maximum desirability, was organized and evaluated.

The mathematical optimization tool with desirability method was employed to prepare co-crystal. The constraints of maximum solubility and maximum % release was imposed on independent variables for optimization. The parameters recommended by the design were concentration of ketoprofen (508.58 mg) & concentration of fumaric acid (228.82 mg) that provide co-crystal with solubility of 56.06 µg/ml (predicted value 56.63 µg/ml) and % drug release 83.35% (predicted value 84.22%). The closer agreement between predicted and observed values indicated the high prognostic ability of the model. Fig. 2 shows the *in vitro* release profile of ketoprofen as pure drug and optimized batch (F4) of co-crystal formulation.

The release rate data of ketoprofen from co-crystal and from drug solution was fitted into several kinetic models to estimate release kinetics and mechanism of drug release. The release rate data was found to be put best into Higuchi model (with R^2 =0.985) of release kinetics. Further, the value of n=0.475 (0.43<n<0.85), release exponent of Korsemeyer and Peppas equation, indicated that the release of ketoprofen from co-crystal occurs by diffusion and erosion of the matrix.

Fourier Transform Infrared Spectroscopy (FT-IR) analysis

FTIR is an excellent analytical technique to study the deviations in the position caused by the vibration modes of the functional groups. This technique reveals the shift in characteristic peaks of drug and coformer due to co-crystal formation involving H bonding between the corresponding functional groups. The spectra of ketoprofen fig. 3 (a) showed characteristic absorption band at 2979.27 cm^{-1} due to –CH stretching. The peak appearing at 1697.76 cm^{-1} can be ascribed to -C=O stretching of acid while peak appearing at 1655.77 cm^{-1} is due to -C=O stretching of ketone. The absorption bands at 1598.67 cm^{-1} (-C=C= stretching), 1442.21 cm^{-1} (-C=O stretching of aromatic ring), 1420.59 cm^{-1} (-C-H deformation of $-CH_3$ asymmetrical) and 1370.04 cm^{-1} (-C-H deformation of $-CH_3$ symmetrical) also appeared. The FTIR spectra of fumaric acid exhibit peaks at 3084.26 cm^{-1}, 1684.31 cm^{-1}, 1422 cm^{-1} ascribed to the -O-H stretching, -C=O stretching vibration and –C-C aromatic stretching, respectively. The FTIR spectra of ket-FACo displayed that -C=O stretching of –COOH group of ketoprofen get shifted from 1697.76 cm^{-1} to 1667.30 cm^{-1} and the peak due to -C=O stretching of fumaric acid at 1655cm^{-1} got disappeared. Therefore, FT-IR analysis confirms the interactions occurring between ketoprofen and fumaric acid. These interactions are essentially hydrogen bonds between the carboxylic group of the fumaric acid and the main functional groups of ketoprofen (-C=O and -O-H) which are able to generate supramolecular heterosynthons.

Powder X-ray diffraction analysis (PXRD)

The powder X-ray diffraction (PXRD) pattern of ketoprofen, fumaric acid and optimized batch of ket-FACo illustrated in fig. 3 (b). The diffraction peaks (and Miller indices) at 2θ of 12.74 (100), 18.52 (200), 22.85 (211), 24.00 (221), 26.32 (222), 28.920 (300), 36.71 (322) and 22.86 (211), 28.92 (300), 29.49 (310), and 30.03 (311) showed crystalline structure of ketoprofen and fumaric acid respectively. The major diffraction peaks at 2θ, 18.57 (200), 23.27 (211), 28.01 (222) and 29.28 (300) were also observed in PXRD spectra of co-crystal that portrayed crystalline nature of resultant product. The distinctive PXRD pattern of the ket-FACo was distinguishable from ketoprofen and fumaric acid, this outcome specifies the formation of a new crystal phase [62].

Differential scanning calorimetry (DSC)

DSC thermograms [fig. 4 (a)], reported that pure ketoprofen showed a sharp endotermic peak at 94.5º that corresponds to its melting point. The peak at 280.4ºC attributed to melting point of fumaric acid. In the thermogram of the prepared co-crystal, peaks were found to be displaced and difference in intensity is also observed from that of its constitutional components indicating the occurrence of weak cohesive forces that bonded together by reversible hydrogen bonding, suggesting the development of co-crystal formation. The thermal behavior of the ket-FACo was prominent, with a different melting transition from that seen with either of the constitutional components; this recommends the formation of a new phase.

Scanning electron microscopy (SEM)

The SEM image of the optimized batch of ket-FACo [fig. 4(c)] depicted good crystalline characteristics. This crystalline character was reinforced by the XRD data, as discussed earlier. The voids over the surface of the co-crystal may brace the imbibition of the solvent and biological fluids and thereby proliferating the solubility and bioavaibility of ketoprofen as estimated.

Nuclear magnetic resonance (NMR) Spectroscopy

NMR spectroscopy is used to characterize the co-crystal by studying the chemical environment of their nuclei and hydrogen bonding and it also offers valuable information regarding interactions. In the NMR pattern of ket-FACo, the carbonyl carbon of ketoprofen corresponding to 196.46 ppm and140.13 ppm has shifted to 196.10 ppm and 142.22 ppm, respectively. A deviation in the carbonyl carbon of carboxylic group in fumaric acid shifted from 166.41 ppm and 140.51 ppm to 175.52 ppm and 137.45 ppm, respectively (Fig. 5). This suggests an interaction between alcoholic group of fumaric acid and –COOH group of ketoprofen in ket-FACo.

Computational studies

The constituents of the co-crystal interact through weak non covalent interactions (NCI) [63] and in order to determine the points of contacts between the ketoprofen and coformer fumaric acid, molecular electrostatic surface potential (MESP) analysis was performed and the extreme positive and negative values from MESP are displayed in fig. 6.

The magnitude of these values signifies that both H-bond donor and acceptor are present in the crystals of both compounds. MESP of ketoprofen exhibits both positive (+53.53 kcal/mol) and negative (-37.40 and -32.94 kcal/mol) extreme values thus proving that it can form intermolecular as well as intramolecular hydrogen bonds during process of co-crystalization. Similarly, fumaric acid displays positive (+69.87 and +69.85 kcal/mol) and negative (-33.5 and -33.46 kcal/mol) extreme values which confirms its hydrogen bonding capability. It has stronger hydrogen bond donor ability due to higher positive extreme value and on the other hand ketoprofen has higher hydrogen bond acceptor ability due to higher negative extreme value. According to Etter's rule [64], there is more probability of interactions between most polar parts of the molecules in a co-crystal. Therefore, these two compounds will pair in the co-crystal through hydrogen bonding. This pairing of these molecules was accomplished by combining two molecules and energy minimization of combined form. The interaction diagram of the molecules in combination is shown in fig. 7 (a, b).

Reduced density gradient (RDG) analysis [fig. 7 (a)] exhibits formation of two hydrogen bonds between two fumaric acid and ketoprofen. Two hydroxyl groups made these two hydrogen bonds (shown as blue colored discs) with two carbonyl oxygen atoms of ketoprofen. Further, van der Waals interactions can be observed between double bond region of fumaric acid and phenyl ring of ketoprofen (shown as green and brown color). The results of RDG calculations are also in line with the MESP predictions. The hydrogen bonding interactions between these two molecules were further confirmed by Hirshfeld surface mapped by electron density with promolecular approximation analysis [fig. 7 (b)]. This calculation shows three regions of high electron density; two are the same as found in RDG analysis while the third is between carbonyl oxygen of fumaric acid and phenyl hydrogen of ketoprofen. These observations are also in agreement with the findings of MESP analysis. The positive parts of one molecule are interacting with negative parts of another molecule.

The geometry of the both molecules individually as well as in combined form was minimized using MOPAC [65] with latest PM7 method choosing value of gnorm as 0.01 after optimization with molecular mechanics method.

Molecular energy and other various properties of the minimized discrete molecules and co-crystal were calculated with Firefly [66] by density functional theory (DFT) taking 6-31G* basis set in B3LYP method. The MESP calculation, RDG analysis and Hirshfeld surface mapped by electron density with promolecular approximation [67] calculations were performed with Multiwfn 3.8 [68] and visualization was done with the help of VMD [69].

Biological evaluation of the co-crystal

In-vitro anti-inflammatory activity

The % protection from denaturation of protein is comparably plotted at different concentration of optimized batch of formulation and pure drug ketoprofen (fig. 8). Egg albumin protein denaturation method displayed concentration dependent anti-inflammatory activity by protecting the protein. Half maximal inhibitory concentration (IC_{50}) values of ketoprofen and optimized formulation was calculated by nonlinear regression analysis. The IC_{50} values for pure drug ketoprofen and optimized formulation was observed to be 556.11 µg/ml and 327.33 µg/ml respectively. Thus it can be inferred that optimized co-crystal formulation is additionally effective as compared to pure drug in generating anti-inflammatory response.

In-vivo anti-inflammatory activity

The improvement in activity of ketoprofen and co-crystal formulation was comparatively assesed by the increase in paw volume of control groups. The paw edema volume (before and after drug administration) and % inhibition of edema at different time interval was convinced and displayed in Table 3. The ketoprofen and co-crystal showed inhibition of paw edema as 49.34±0.18% and 60.39±0.15 at the end of 5 h, respectively thus demonstrating quick onset of action by co-crystal in contrast with the pure drug ketoprofen.

Statical Analysis:- Data was compared by ANOVA followed by Tukey's test. The p value is <0.0005 is considered as significant.

Table 3. Effect of ketoprofen and optimized batch of ket-FACo formulation on the paw edema induced by carrageenan in Wistar rats.

Time (min)	Paw volume	(mm)		Inibition (%)	
	Control	Pure drug	Co-crystal	Pure drug	Co-crystal
60	4.25±0.07	4.12±0.03*	4.02±0.09*	1.05±0.03	5.17±0.08#
120	4.54±0.10	3.86±0.06*	3.53±0.04*	10.97±0.01	16.65±0.09#
180	4.96±0.014	3.48±0.04*	3.22±0.06*	29.83±0.03	35.08±0.27#
240	5.49±0.06	3.31±0.05*	3.04±0.04*	39.70±0.10	44.62±0.03#
300	6.11±0.022	3.09±0.03*	2.42±0.035*	49.34±0.18	60.39±0.15#

*All values are expressed as mean ± S.D., n=6. *Significant (p<0.05) compared to control. #Significant (p<0.05) compared to pure drug (ketoprofen).*

Analgesic activity

The results of the % analgesic activity (PAA) of test, reference and control group are shown in Table 4. The PAA (equation 8) was comparatively evaluated for Ket-FACo and pure drug based on its potential to suppress pain. Ket-FACo showed significant effect in enhancing the pain thershold to a certain extent when compared to that of drug (ketoprofen), thus, stipulating that an improvement in solubility further tweaked the pharmacological response.

Table 4. % Analgesic effect of ketoprofen and optimized batch of Ket-FACo by tail flick method in mice.

Treatment	PAA					
	0h	1h	2h	3h	4h	5h
Standard (ketoprofen)	0.06±0.020	31.30±0.71*	35.18±0.12*	42.36±0.17*	50.93±0.14*	71.96±0.17*
Test (Ket-FACo)	0.09±0.021	32.14±0.24*	50.44±0.14*#	60.23±0.18*#	65.41±0.12*#	75.68±0.22*#
Control (vehicle)	0.01±0.012	0.91±0.19	1.32±0.02	0.83±0.10	1.1±0.20	0.021±0.03

*All values are expressed as mean ± S.D., n=6.*Significant ($p<0.05$) compared to control.#Significant ($p<0.05$) compared to pure drug (ketoprofen).*

Conclusion

The present study demonstrated the effectiveness of ketoprofen co-crystal towards improved solubility and anti-inflammatory activity. Co-crystal of ketoprofen with fumaric acid prepared via simple solvent-assisted grinding technique were systematically characterized through DSC, PXRD, FTIR and NMR studies was further evaluated for *in-vitro* and *in-vivo* anti-inflammatory and analgesic activities. The solubility and % drug release of different batches of co-crystal was found to be between 30.68–57.44 µg/ml and 62.21–83.68%, respectively. The IC_{50} values for pure drug ketoprofen and optimized formulation was observed to be 556.11 µg/ml and 327.33 µg/ml respectively. Thus it can be inferred that optimized co-crystal formulation is additionally effective as compared to pure drug in generating anti-inflammatory response. Thus, the reported co-crystal have important implications for the use of co-crystallization approach to improve drugs solubility and efficacy of BCS- II drugs.

Declarations

Consent for Publication

Not applicable.

Availability of Data and Materials

All the data is available in the manuscript.

Author Contributions

Sunita Devi- Conceptualization, Writing – Original Draft Preparation; Meenakshi Bhatia- Conceptualization, Supervision; Ashwini Kumar- Review & Editing, Software; Vikas Verma- Writing – Review & Editing; Snehlata Yadav– Review & Editing, Data Curation.

Ethical Approval and Consent to Participate

This investigation is approved by IAEC, Guru Jambheshwar University of Science and Technology, Hisar, India under CPCSEA reg. no-IAEC/2021/10-19.

Funding

None.

Acknowledgement

None.

Conflict of Interest

The authors declare that there is no conflict of interest.

References

1. Rasenack N, Müller BW. Micron-size drug particles: common and novel micronization techniques. Pharmaceutical development technology. 2004;9(1):1–13. https://doi.org/10.1081/PDT-120027417.
2. Jain NK, Gupta U. Application of dendrimer–drug complexation in the enhancement of drug solubility and bioavailability. Expert Opin Drug Metab Toxicol. 2008;4(8):1035–52. https://doi.org/10.1517/17425255.4.8.1035.
3. Oprean C, Mioc M, Csányi E, Ambrus R, Bojin F, Tatu C, Soica C. Improvement of ursolic and oleanolic acids' antitumor activity by complexation with hydrophilic cyclodextrins. Biomed Pharmacother. 2016;83:1095–104. https://doi.org/10.1016/j.biopha.2016.08.030.
4. Medarević D, Kachrimanis K, Djurić Z, Ibrić S. Influence of hydrophilic polymers on the complexation of carbamazepine with hydroxypropyl-β-cyclodextrin. Eur J Pharm Sci. 2015;78:273–85. https://doi.org/10.1016/j.ejps.2015.08.001.
5. Bhatia M, Devi R. (2019). Enhanced Solubility and Drug Release of Ketoprofen Using Lyophilized Bovine Serum Albumin Solid Dispersion. ACTA Pharmaceutica Sciencia, 57(1), DOI:10.23893/1307-2080.APS.05703.
6. Bhatia M, Devi S, Development. Characterisation and Evaluation of PVP K-30/PEG Solid Dispersion Containing Ketoprofen. *ACTA Pharmaceutica Sciencia*, *58*(1), DOI: 10.23893/1307-2080.APS.05806.
7. Strickley RG. Solubilizing excipients in oral and injectable formulations. Pharmaceutical research. 2004;21(2):201–30. https://doi.org/10.1023/B:PHAM.0000016235.32639.23.
8. Witzigmann D, Kulkarni JA, Leung J, Chen S, Cullis PR, van der Meel R. Lipid nanoparticle technology for therapeutic gene regulation in the liver. Adv Drug Deliv Rev. 2020. https://doi.org/10.1016/j.addr.2020.06.026.
9. Wang Y, Zheng Z, Wang K, Tang C, Liu Y, Li J. Prebiotic carbohydrates: Effect on physicochemical stability and solubility of algal oil nanoparticles. Carbohydrate polymers. 2020;228:115372. https://doi.org/10.1016/j.carbpol.2019.115372.

10. Dhiman P, Bhatia M. Microwave assisted quaternized cyclodextrin grafted chitosan (QCD-g-CH) nanoparticles entrapping ciprofloxacin. J Polym Res. 2021;28(5):1–14. DOIhttps://doi.org/10.1007/s10965-021-02535-9.
11. Dhiman P, Bhatia M. (2021). Ketoconazole loaded quaternized chitosan nanoparticles-PVA film: preparation and evaluation. Polym Bull, 1–19. DOI:https://doi.org/10.1007/s00289-020-03500-0.
12. Aloisio C, Bueno MS, Ponte MP, Paredes A, Palma SD, Longhi M. Development of solid self-emulsifying drug delivery systems (SEDDS) to improve the solubility of resveratrol. Therapeutic delivery. 2019;10(10):626–41. https://doi.org/10.4155/tde-2019-0054.
13. Czajkowska-Kośnik A, Szekalska M, Amelian A, Szymańska E, Winnicka K. (2015). Development and evaluation of liquid and solid self-emulsifying drug delivery systems for atorvastatin. *Molecules*, *20*(12), 21010–21022, **https**://**doi**.**org**/**10**.**3390**/**molecules201219745**.
14. Kadu PJ, Kushare SS, Thacker DD, Gattani SG. Enhancement of oral bioavailability of atorvastatin calcium by self-emulsifying drug delivery systems (SEDDS). Pharm Dev Technol. 2011;16(1):65–74. https://doi.org/10.3109/10837450903499333.
15. Gwak HS, Choi JS, Choi HK. Enhanced bioavailability of piroxicam via salt formation with ethanolamines. International journal of pharmaceutics. 2005;297(1–2):156–61. https://doi.org/10.1016/j.ijpharm.2005.03.016.
16. Coimbra, M., Isacchi, B., van Bloois, L., Torano, J. S., Ket, A., Wu, X., … Schiffelers,R. M. (2011). Improving solubility and chemical stability of natural compounds for medicinal use by incorporation into liposomes. *International journal of pharmaceutics*, *416*(2), 433–442, https://doi.org/10.1016/j.ijpharm.2011.01.056.
17. Zhuang, C. Y., Li, N., Wang, M., Zhang, X. N., Pan, W. S., Peng, J. J., … Tang, X.(2010). Preparation and characterization of vinpocetine loaded nanostructured lipid carriers (NLC) for improved oral bioavailability. *International journal of pharmaceutics*, *394*(1–2), 179–185, https://doi.org/10.1016/j.ijpharm.2010.05.005.
18. Sun M, Nie S, Pan X, Zhang R, Fan Z, Wang S. Quercetin-nanostructured lipid carriers: characteristics and anti-breast cancer activities in vitro. Colloids Surf B. 2014;113:15–24. https://doi.org/10.1016/j.colsurfb.2013.08.032.
19. Jornada DH, dos Santos Fernandes GF, Chiba DE, De Melo TRF, Santos D, J. L., & Chung MC. (2016). The prodrug approach: a successful tool for improving drug solubility. *Molecules*, *21*(1), 42, **https**://**doi**.**org**/**10**.**3390**/**molecules21010042**.
20. Bahr MN, Angamuthu M, Leonhardt S, Campbell G, Neau SH. Rapid screening approaches for solubility enhancement, precipitation inhibition and dissociation of a cocrystal drug substance using high throughput experimentation. Journal of Drug Delivery Science Technology. 2021;61:102196. https://doi.org/10.1016/j.jddst.2020.102196.
21. Mannava MC, Gunnam A, Lodagekar A, Shastri NR, Nangia AK, Solomon KA. Enhanced solubility, permeability, and tabletability of nicorandil by salt and cocrystal formation. CrystEngComm. 2021;23(1):227–37. DOI:10.1039/D0CE01316A.
22. Pantwalawalkar J, More H, Bhange D, Patil U, Jadhav N. Novel curcumin ascorbic acid cocrystal for improved solubility. Journal of Drug Delivery Science Technology. 2021;61:102233. https://doi.org/10.1016/j.jddst.2020.102233.
23. Cavanagh KL, Kuminek G, Rodríguez-Hornedo N. Cocrystal Solubility Advantage and Dose/Solubility Ratio Diagrams: A Mechanistic Approach To Selecting Additives and Controlling Dissolution–Supersaturation–

Precipitation Behavior. Mol Pharm. 2020;17(11):4286–301. https://doi.org/10.1021/acs.molpharmaceut.0c00713.

24. Kimoto K, Yamamoto M, Karashima M, Hohokabe M, Takeda J, Yamamoto K, Ikeda Y. (2020). Pharmaceutical cocrystal development of TAK-020 with enhanced oral absorption. *Crystals*, *10*(3), 211, **https**://**doi**.**org**/**10**.**3390**/**cryst10030211**.
25. Guo C, Zhang Q, Zhu B, Zhang Z, Bao J, Ding Q, Mei X. Pharmaceutical Cocrystals of Nicorandil with Enhanced Chemical Stability and Sustained Release. Cryst Growth Des. 2020;20(10):6995–7005. https://doi.org/10.1021/acs.cgd.0c01043.
26. Sarraguça MC, Ribeiro PR, Santos D, A. O., & Lopes JA. Batch statistical process monitoring approach to a cocrystallization process. Journal of pharmaceutical sciences. 2015;104(12):4099–108. https://doi.org/10.1002/jps.24623.
27. Soares FL, Carneiro RL. Green synthesis of ibuprofen–nicotinamide cocrystals and in-line evaluation by Raman spectroscopy. Cryst Growth Des. 2013;13(4):1510–7. https://doi.org/10.1021/cg3017112.
28. Maheshwari C, André V, Reddy S, Roy L, Duarte T, Rodríguez-Hornedo N. Tailoring aqueous solubility of a highly soluble compound via cocrystallization: effect of coformer ionization, pH max and solute–solvent interactions. Cryst Eng Comm. 2012;14(14):4801–11. https://doi.org/10.1039/C2CE06615G.
29. Sathisaran I, Dalvi SV. Engineering cocrystals of poorly water-soluble drugs to enhance dissolution in aqueous medium. Pharmaceutics. 2018;10(3):108. https://doi.org/10.3390/pharmaceutics10030108.
30. Amin MA, Osman SK, Aly UF. (2013). Preparation and characterization of ketoprofen nanosuspension for solubility and dissolution velocity enhancement. *International Journal of Pharma and Bio Sciences2013*, *4*, 768–780.
31. Yadav PS, Kumar V, Singh UP, Bhat HR, Mazumder B. Physicochemical characterization and in vitro dissolution studies of solid dispersions of ketoprofen with PVP K30 and d-mannitol. Saudi Pharmaceutical Journal. 2013;21(1):77–84. https://doi.org/10.1016/j.jsps.2011.12.007.
32. Nikumbh KV, Sevankar SG, Patil MP. Formulation development, in vitro and in vivo evaluation of microemulsion-based gel loaded with ketoprofen. Drug Deliv. 2015;22(4):509–15. https://doi.org/10.3109/10717544.2013.859186.
33. Ambala R, Vemula SK. Formulation and characterization of ketoprofen emulgels. Journal of Applied Pharmaceutical Science. 2015;5(7):112–7. DOI:10.7324/JAPS.2015.50717.
34. Attia MF, Anton N, Khan IU, Serra CA, Messaddeq N, Jakhmola A, Vandamme T. One-step synthesis of iron oxide polypyrrole nanoparticles encapsulating ketoprofen as model of hydrophobic drug. Int J Pharm. 2016;508(1–2):61–70. https://doi.org/10.1016/j.ijpharm.2016.04.073.
35. Shah PP, Desai PR, Singh M. Effect of oleic acid modified polymeric bilayered nanoparticles on percutaneous delivery of spantide II and ketoprofen. Journal of controlled release. 2012;158(2):336–45. https://doi.org/10.1016/j.jconrel.2011.11.016.
36. Gul R, Ahmed N, Ullah N, Khan MI, Elaissari A. Biodegradable ingredient-based emulgel loaded with ketoprofen nanoparticles. AAPS PharmSciTech. 2018;19(4):1869–81. https://doi.org/10.1208/s12249-018-0997-0.
37. Kheradmandnia S, Vasheghani-Farahani E, Nosrati M, Atyabi F. Preparation and characterization of ketoprofen-loaded solid lipid nanoparticles made from beeswax and carnauba wax. Nanomed Nanotechnol Biol Med. 2010;6(6):753–9. https://doi.org/10.1016/j.nano.2010.06.003.

38. Cirri M, Bragagni M, Mennini N, Mura P. Development of a new delivery system consisting in “drug–in cyclodextrin–in nanostructured lipid carriers” for ketoprofen topical delivery. Eur J Pharm Biopharm. 2012;80(1):46–53. https://doi.org/10.1016/j.ejpb.2011.07.015.
39. Xi MM, Wang XY, Fang KQ, Gu Y. Study on the characteristics of pectin–ketoprofen for colon targeting in rats. International journal of pharmaceutics. 2005;298(1):91–7. https://doi.org/10.1016/j.ijpharm.2005.04.012.
40. Kluge J, Fusaro F, Mazzotti M, Muhrer G. Production of PLGA micro-and nanocomposites by supercritical fluid extraction of emulsions: II. Encapsulation of Ketoprofen. J Supercrit Fluids. 2009;50(3):336–43. https://doi.org/10.1016/j.supflu.2009.05.002.
41. Vittal GV, Deveswaran R, Bharath S, Basavaraj BV, Madhavan V. Formulation and characterization of ketoprofen liquisolid compacts by Box-Behnken design. International journal of pharmaceutical investigation. 2012;2(3):150. doi:10.4103/2230-973X.104398.
42. Perpétuo GL, Chierice GO, Ferreira LT, Fraga-Silva TFC, Venturini J, Arruda MSP, Castro RAE. A combined approach using differential scanning calorimetry with polarized light thermomicroscopy in the investigation of ketoprofen and nicotinamide cocrystal. Thermochim Acta. 2017;651:1–10. https://doi.org/10.1016/j.tca.2017.02.014.
43. Evora AO, Bernardes CE, Piedade MFM, Conceição AC, & Minas da Piedade, M. E. (2019). Energetics of glycine cocrystal or salt formation with two regioisomers: fumaric acid and maleic acid. *Crystal Growth & Design*, *19*(9),5054–5064, https://doi.org/10.1021/acs.cgd.9b00379.
44. Fernandes RP, Nascimento do, Carvalho ALCS, Teixeira ACS, Ionashiro JA, M., & Caires FJ. Mechanochemical synthesis, characterization, and thermal behavior of meloxicam cocrystals with salicylic acid, fumaric acid, and malic acid. J Therm Anal Calorim. 2019;138(1):765–77. https://doi.org/10.1007/s10973-019-08118-7.
45. Gonnade RG, Iwama S, Mori Y, Takahashi H, Tsue H, Tamura R. Observation of efficient preferential enrichment phenomenon for a cocrystal of (DL)-phenylalanine and fumaric acid under nonequilibrium crystallization conditions. Cryst Growth Des. 2011;11(2):607–15. https://doi.org/10.1021/cg1015274.
46. Du Y, Fang HX, Zhang Q, Zhang HL, Hong Z. Spectroscopic investigation on cocrystal formation between adenine and fumaric acid based on infrared and Raman techniques. Spectrochim Acta Part A Mol Biomol Spectrosc. 2016;153:580–5. https://doi.org/10.1016/j.saa.2015.09.020.
47. Du Y, Cai Q, Xue J, Zhang Q, Qin D. Structural investigation of the cocrystal formed between 5-fluorocytosine and fumaric acid based on vibrational spectroscopic technique. Spectrochim Acta Part A Mol Biomol Spectrosc. 2017;178:251–7. https://doi.org/10.1016/j.saa.2017.02.004.
48. Manoj K, Takahashi H, Iwama S, Gonnade RG, Tsue H, Tamura R. Crystal structure analysis of highly efficient chiral resolution of (RS)-arginine-fumaric acid cocrystal under preferential enrichment conditions. J Mol Struct. 2021;1245:131073. https://doi.org/10.1016/j.molstruc.2021.131073.
49. Yang D, Cao J, Jiao L, Yang S, Zhang L, Lu Y, Du G. Solubility and stability advantages of a new cocrystal of berberine chloride with fumaric acid. ACS omega. 2020;5(14):8283–92. https://doi.org/10.1021/acsomega.0c00692.
50. Kacso I, Rus LM, Martin F, Miclaus M, Filip X, Dan M. Solid-state compatibility studies of Ketoconazole-Fumaric acid co-crystal with tablet excipients. J Therm Anal Calorim. 2021;143(5):3499–506. https://doi.org/10.1007/s10973-020-09340-4.
51. Bhogala BR, Basavoju S, Nangia A. (2005). Tape and layer structures in cocrystals of some di-and tricarboxylic acids with 4, 4'-bipyridines and isonicotinamide. From binary to ternary cocrystals.

CrystEngComm, *7*(90), 551–562, **https**://**doi**.**org**/**10**.**1039**/**B509162D**.

52. Sarkar A, Rohani S. (2015). Cocrystals of acyclovir with promising physicochemical properties. *Journal of pharmaceutical sciences*, *104*(1), 98–105, **https**://**doi**.**org**/**10**.**1002**/**jps**.**24248**.
53. Gautam MK, Besan M, Pandit D, Mandal S, Chadha R. Cocrystal of 5-fluorouracil: Characterization and evaluation of biopharmaceutical parameters. AAPS PharmSciTech. 2019;20(4):149. https://doi.org/10.1208/s12249-019-1360-9.
54. Semalty A, Semalty M, Singh D, Rawat MSM. Preparation and characterization of phospholipid complexes of naringenin for effective drug delivery. J Incl Phenom Macrocyclic Chem. 2010;67(3–4):253–60. DOI 10.1007/s10847-009-9705-8.
55. Luo Y, Chen S, Zhou J, Chen J, Tian L, Gao W, Zhou Z. Luteolin cocrystals: Characterization, evaluation of solubility, oral bioavailability and theoretical calculation. Journal of Drug Delivery Science Technology. 2019;50:248–54. https://doi.org/10.1016/j.jddst.2019.02.004.
56. Chavan RR, Hosamani KM. (2018). Microwave-assisted synthesis, computational studies and antibacterial/anti-inflammatory activities of compounds based on coumarin-pyrazole hybrid. *Royal Society open science*, *5*(5), 172435, **https**://**doi**.**org**/**10**.**1098**/**rsos**.**172435**.
57. Bhatia M, Rohilla S. Formulation and optimization of quinoa starch nanoparticles: Quality by design approach for solubility enhancement of piroxicam. Saudi Pharmaceutical Journal. 2020;28(8):927–35. https://doi.org/10.1016/j.jsps.2020.06.013.
58. Shandil A, Yadav M, Sharma N, Nagpal K, Jindal DK, Deep A, Kumar S. Targeting keratinocyte hyperproliferation, inflammation, oxidative species and microbial infection by biological macromolecule-based chitosan nanoparticle-mediated gallic acid–rutin combination for the treatment of psoriasis. Polym Bull. 2020;77(9):4713–38. https://doi.org/10.1007/s00289-019-02984-9.
59. Khullar R, Kumar D, Seth N, Saini S. Formulation and evaluation of mefenamic acid emulgel for topical delivery. Saudi pharmaceutical journal. 2012;20(1):63–7. https://doi.org/10.1016/j.jsps.2011.08.001.
60. Kulkarni SK. Heat and other physiological stress-induced analgesia: catecholamine mediated and naloxone reversible response. Life sciences. 1980;27(3):185–8. https://doi.org/10.1016/0024-3205(80)90136-8.
61. Olbert M, Gdula-Argasińska J, Nowak G, Librowski T. Beneficial effect of nanoparticles over standard form of zinc oxide in enhancing the anti-inflammatory activity of ketoprofen in rats. Pharmacological Reports. 2017;69(4):679–82.
62. Sun S, Zhang X, Cui J, Liang S. (2020). Identification of the Miller indices of a crystallographic plane: a tutorial and a comprehensive review on fundamental theory, universal methods based on different case studies and matters needing attention. *Nanoscale*, *12*(32), 16657–16677, **https**://**doi**.**org**/**10**.**1039**/**D0NR03637D**.
63. Yadav AV, Shete AS, Dabke AP, Kulkarni PV, Sakhare SS. Co-Crystals: A Novel Approach to Modify Physicochemical Properties of Active Pharmaceutical Ingredients. Indian J Pharm Sci. 2009 Jul-Aug;71(4):359–70.
64. Etter MC. Encoding and decoding hydrogen-bond patters of organic compounds. Acc Chem Res. 1990;23:120–6.
65. MOPAC2016, Version: 20.225W, James J. P. Stewart, Stewart Computational Chemistry, web: HTTP://OpenMOPAC.net. Days left: 237.
66. Alex A, Granovsky. Firefly version 8, www http://classic.chem.msu.su/gran/firefly/index.html.

67. Tian Lu F, Chen. Quantitative analysis of molecular surface based on improved Marching Tetrahedra algorithm. J Mol Graph Model. 2012;38:314–23. DOI:10.1016/j.jmgm.2012.07.004.
68. Tian Lu F, Chen. J Comput Chem. 2012;33:580–92.
69. Humphrey W, Dalke A, Schulten K. VMD - Visual Molecular Dynamics. J Molec Graphics. 1996;14(1):33–8.

Figures

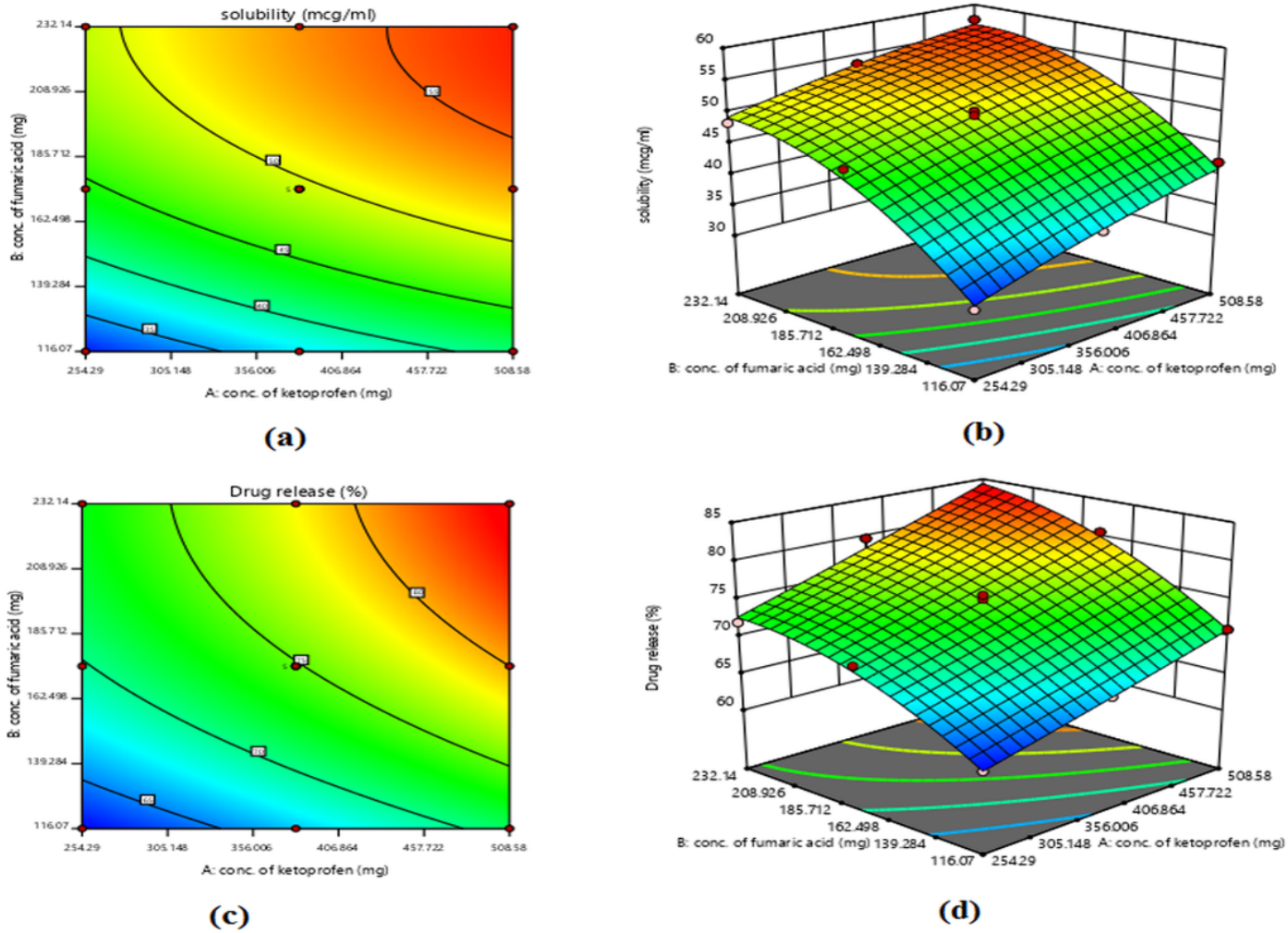

Figure 1

Contour plots (a, c) and response surface plots (b, d) showing the effect of concentration of ketoprofen & fumaric acid on solubility (Y1) and drug release (Y2) respectively.

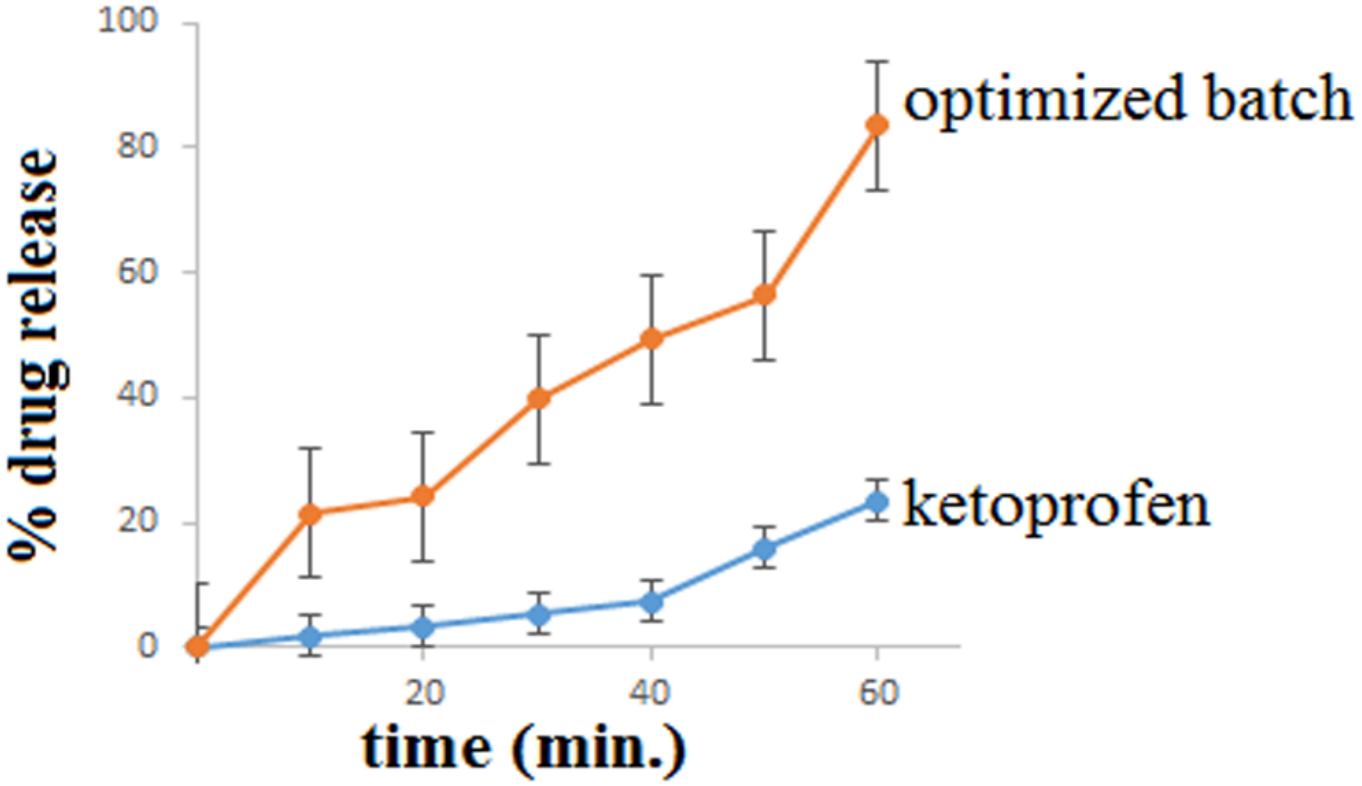

Figure 2

In-vitro release profile of ketoprofen and optimized batch of ket-FACo.

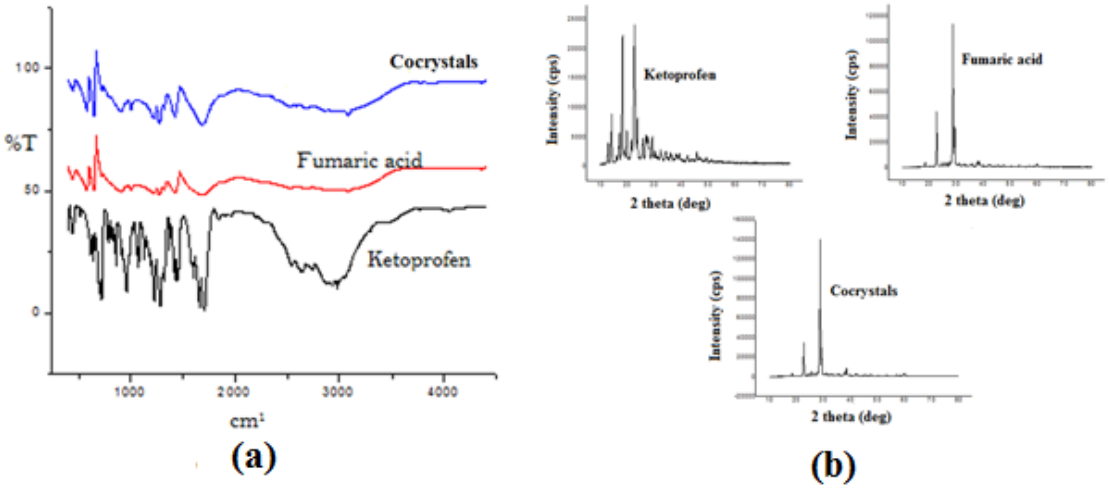

Figure 3

FTIR spectra (a) and (b) XRD patterns of Ketoprofen, Fumaric acid and optimized batch of ket-FACo.

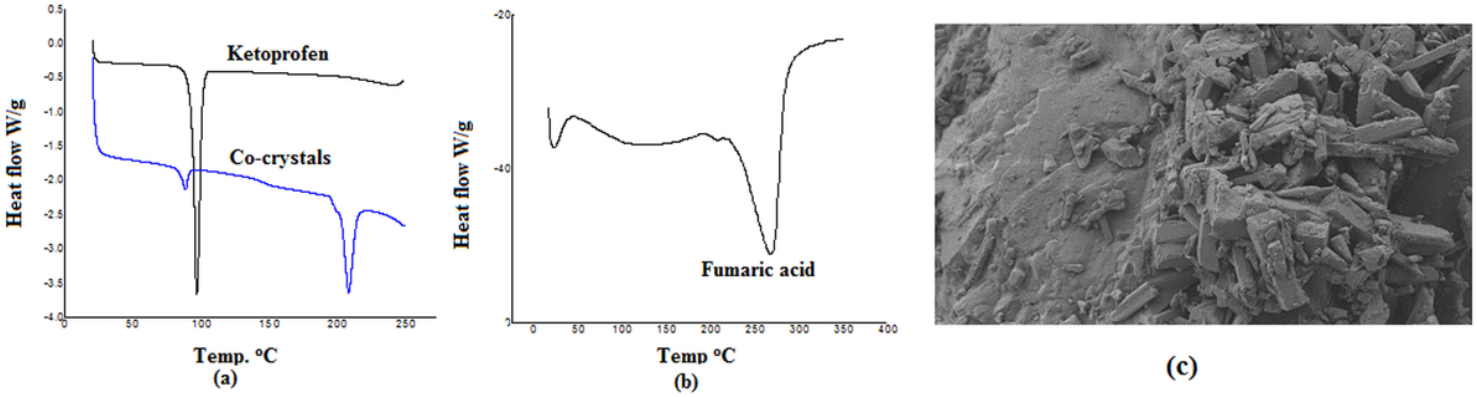

Figure 4

DSC curves of ketoprofen, optimized batch of Ket-FACo (a) and fumaric acid (b) and SEM image of optimized batch of ket-FACo (c).

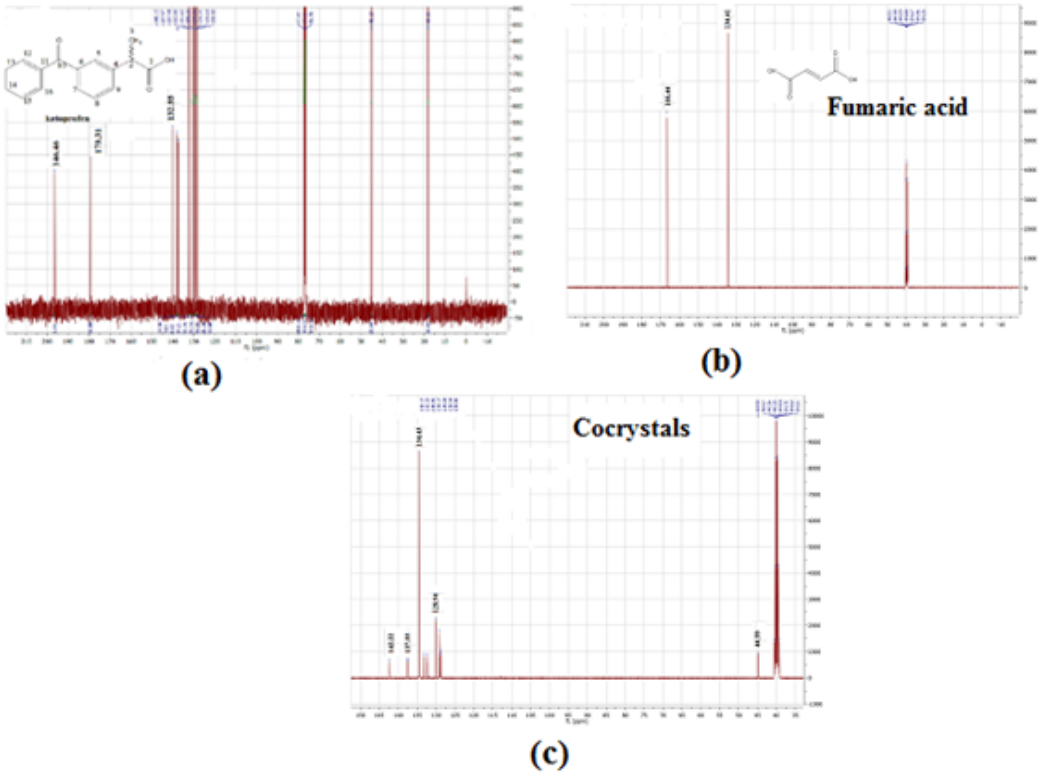

Figure 5

NMR spectra of ketoprofen (a), fumaric acid (b) and optimized batch of ket-FACo (c).

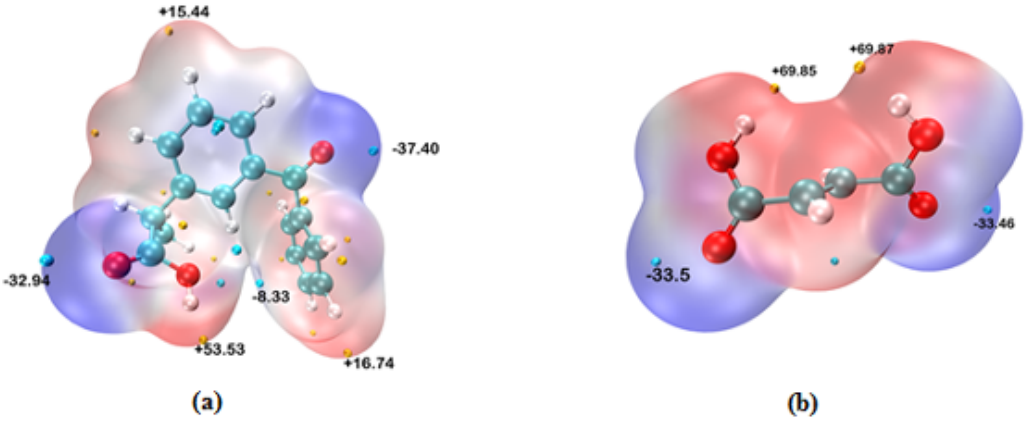

Figure 6

Extreme values (positive and negative values in kcal/mol) from MESP of individual ketoprofen and fumaric acid.

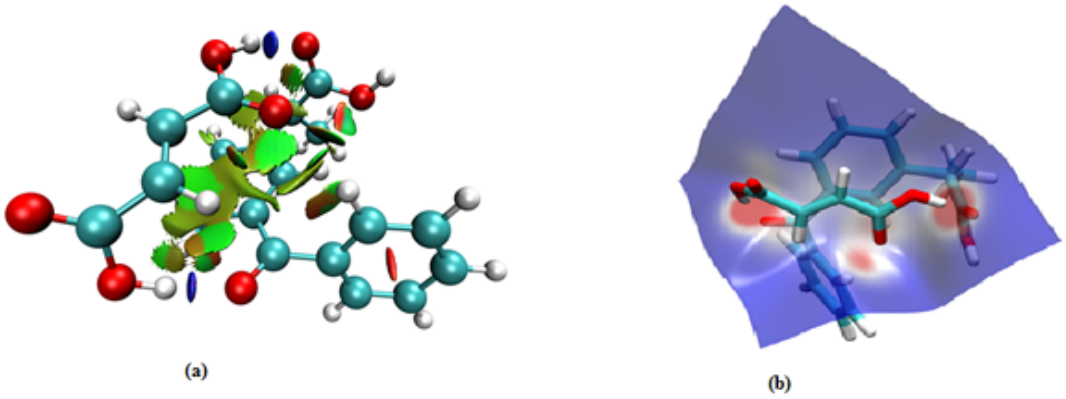

Figure 7

Non-covalent interactions between ketoprofen and fumaric acid (a) and Hirshfeld surface mapped by electron density with promolecular approximation showing hydrogen bonding between ketoprofen and fumaric acid (b). (Red: high electron density, White: low electron density, Blue: zero electron density).

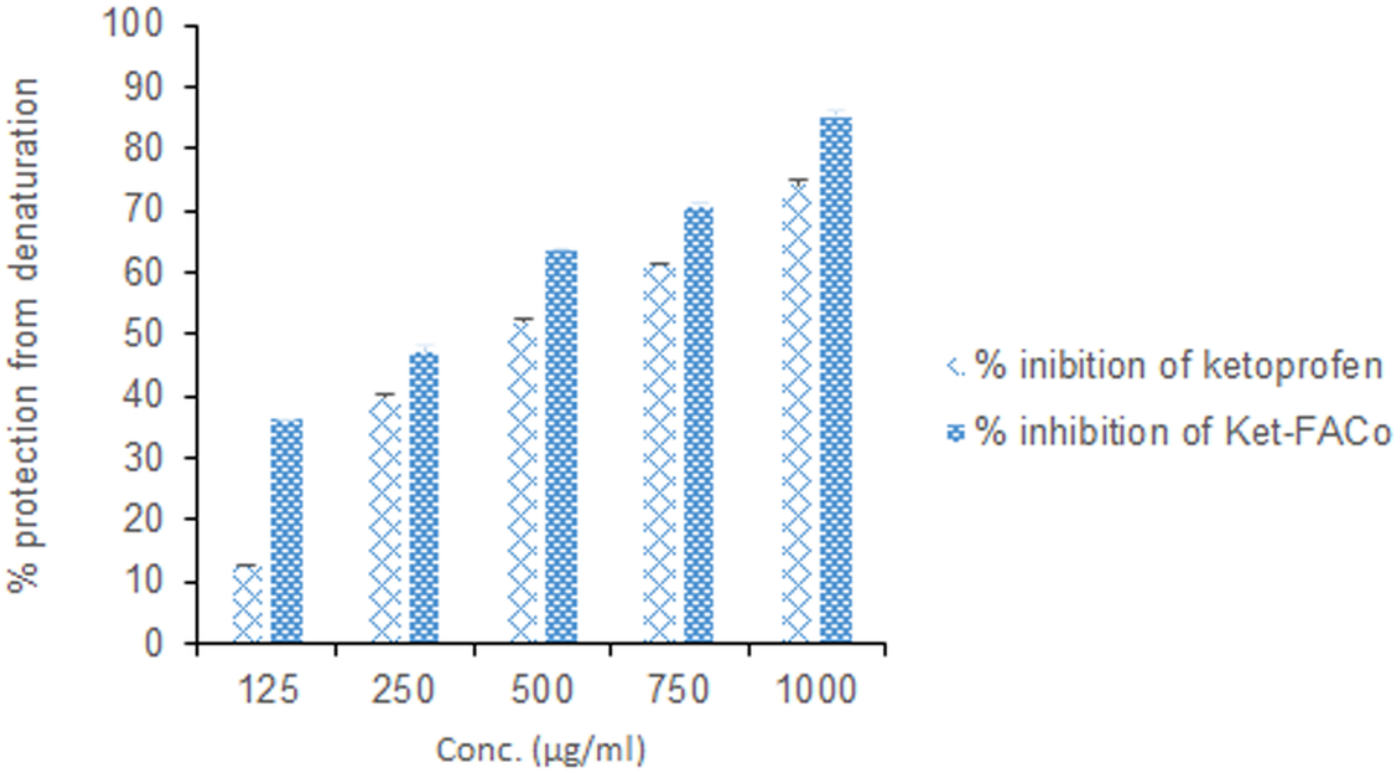

Figure 8

% protection from protein denaturation of ketoprofen and optimized formulation.

Supplementary Files

This is a list of supplementary files associated with this preprint. Click to download.

- graphicalabstractKETFACOCopy.tif